Proceedings of the XII International Symposium on Dynamic Problems of Mechanics (DINAME 2007),
P.S.Varoto and M.A.Trindade (editors), ABCM, Ilhabela, SP, Brazil, February 26 - March 2, 2007

Design and Realization of Humanoid Robots at AM-TUM

Heinz Ulbrich, Thomas Buschmann and Sebastian Lohmeier

Institute of Applied Mechanics, Technische Universität München, Bolzmannstrasse 15, 85748 Garching, GERMANY,
{ulbrich,buschmann,lohmeier}@amm.mw.tum.de

Abstract: This paper presents the design and realization of the humanoid robots JOHNNIE and LOLA at the Institute of Applied Mechanics, Technische Universität München (AM-TUM). The presentation focuses on the new robot LOLA and the differences in it's hardware design compared to JOHNNIE's. Furthermore, the simulation used for developing both robot hardware and control software is presented.

Keywords: Humanoid robots, lightweight construction, hardware design, simulation

INTRODUCTION

Driven by the rapid development of actuator and computer technology, an increasing number of more and more sophisticated humanoid robots is being developed (Hirai et al., 1998, Nishiwaki et al., 2002b, Ishida et al., 2003, Kaneko et al., 2004, Ogura et al., 2004, Kim et al., 2005). Bipedal walking is considered to be one of the core technologies for a humanoid robot. While most biped robots are able to achieve reliable dynamic walking, walking speeds still are slow for most robots when compared with human walking. Recently, *ASIMO* was reported to run as fast as 6 km/h (Honda, 2005), but almost no details on the controller and hardware design have been published yet. However, *ASIMO* can be seen as proof that a fully actuated biped with a stiff structure is capable of fast locomotion. Other recent developments look very promising as well. The top speed of *HRP-2* is 2.5 km/h (Kaneko et al., 2004) and there are attempts to realize a running motion with both feet lifting off the ground (Kajita et al., 2004). Our robot *JOHNNIE* (Fig. 1) has reached a maximum of 2.4 km/h (Pfeiffer et al., 2004).

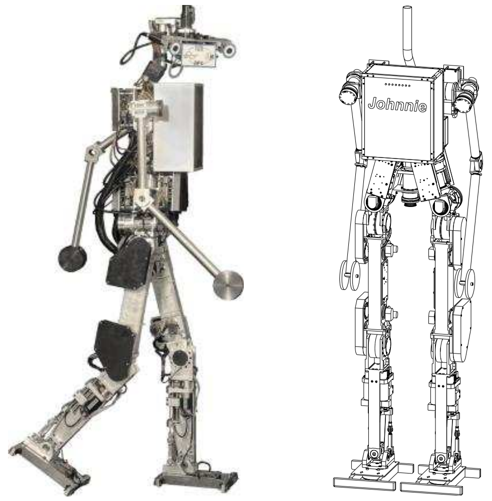

Figure 1 – The biped robot Johnnie.

Based on the experiences with *JOHNNIE* the humanoid robot *LOLA* with enhanced performance is being developed. The goal of our current project is to realize a fast, human-like walking motion, i. e. a significant increase in walking speed, more flexible gait patterns and increased autonomy. Besides the challenging control problems inherent in fast walking, research effort is also required for the robot hardware. Obviously, the robot must be able to provide the required velocities at a high dynamic response. Then there is the important issue of choosing the best kinematic configuration. And, generally speaking, the weight of the robot has to be kept at a minimum which must be balanced with the requirements for powerful actuators and high structural stiffness.

The paper is organized as follows. First, the kinematic structure of the robots *JOHNNIE* and *LOLA* is presented. The following section gives a short overview of the dimensioning of the robot hardware including motor and gear selection. Next, the modular joint concept for *LOLA* is introduced, followed by a brief overview of the simulation tool developed for the robot's hardware and controller design. Finally, the electronics concept using decentralized joint controllers is presented.

KINEMATIC STRUCTURE OF JOHNNIE AND LOLA

Our special interest is the realization of a fast, human-like walking motion. Therefore the kinematic configuration of the robots is mainly determined by the characteristics of human walking. The robot *JOHNNIE* (cf. Fig. 1) has a total of 17 actuated degrees of freedom (DoF): 12 for the legs (6 each), 1 for the torso and 4 for the Arms. Its physical dimensions are based on anthropometric data and correspond with an 180 cm tall adult. For *LOLA* 5 new joints are introduced in addition to the 17 DoF of *JOHNNIE*—elbow joints, a 2-DoF waist joint and toe joints, giving the robot a total of 22 DoF. The kinematic structure and the CAD model of the *LOLA* are shown in Fig. 2.

Elbow joint Especially at higher walking speeds a reciprocal arm swing is of great importance to reduce the yaw moment between foot and ground (Perry, 1992). Arm motion is used only to avoid slipping, so full arms with hands are not needed but the arms are equipped with additional masses at their ends. However, introducing elbow joints is advantageous for fast walking, since they permit translational arm swing. This is more effective than a purely rotational motion. In addition, the moment of inertia of the arms can be adjusted by using the elbow and shoulder (roll axis) joints.

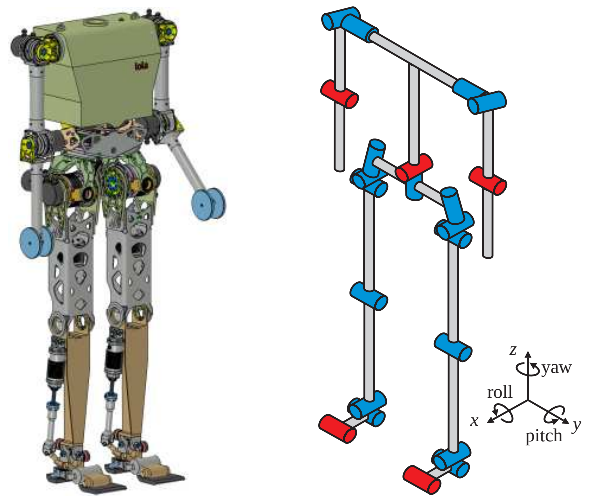

Figure 2 – CAD model and joint structure of the robot *LOLA*. The newly introduced DoF are marked in red.

2-DoF waist Joint A 2-DoF waist allows torso and pelvis to roll and yaw independently which allows to increase step length and provides more mobility for lateral motions. The roll axis facilitates walking with a straight stance leg at nearly constant height of the center of gravity (Perry, 1992). The yaw axis can further be used to compensate for the yaw moment between foot and ground. *WABIAN-2 LL* has a similar waist joint configuration (Ogura et al., 2004).

Hip joint The 3-DoF hip joint is of particular interest since it connects leg and pelvis and its overall stiffness considerably influences the walking performance. The hip joint shown in Fig. 3(a) is actuated by three serial drives composing a spherical joint with axes intersecting at one point. Its compact design allows for keeping anthropometric proportions throughout the robot including the height of the torso. For better power distribution among the three hip drives, the yaw axis is inclined 15° to the vertical axis, (cf. Gienger, 2005).

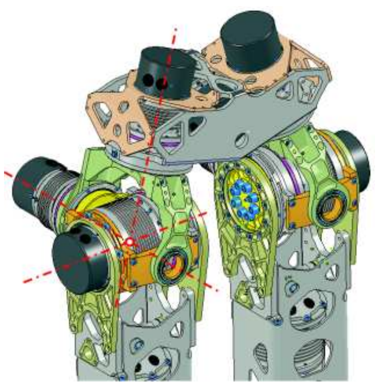

(a) Hip joint with intersecting axes

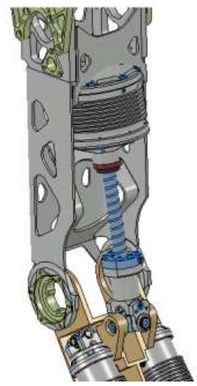

(b) Knee joint with linear actuator

Figure 3 – Hip joint and knee joint

Knee joint with linear actuator Torques and velocities of knee and hip pitch axis are similar, so that the intention of a modular design originally implied the use of identical drives. However, using the hip joint module for the knee is problematic because its mass would unacceptably increase the thigh moment of inertia. In turn a large part of the enhanced hip joint output would be spent on accelerating a heavier knee. Because of positive experience with ballscrews in the ankle joints of *JOHNNIE* (Gienger et al., 2001) we went for the same actuation principle for the knees. The "muscle-like" mechanism is shown schematically on the left of Fig. 4, the actual mechanical configuration is depicted in Fig. 3(b). Thus, a better mass distribution in the hip-thigh area is achieved and *LOLA*'s thigh's moment of inertia is

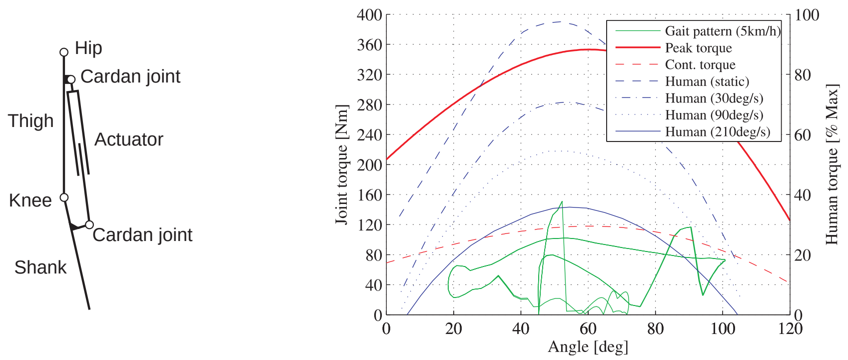

Figure 4 – Left: Mechanism employed for the the knee joint. Right: Torque and speed requirements of knee joint, human torque capacity from Perry, 1992.

only marginally higher than *JOHNNIE*'s. Thus, the driving power of the knee could be enhanced without decreasing the hip joint's performance. The mechanism has nonlinear transfer behavior which is advantageous for typical gait patterns since the torque markedly depends on the link position and has its maximum at around 50°. Figure 4 shows the torque requirements in the knee for a walking speed of 5 km/h compared to the torque capacity of the drive and the velocity dependent capacity of the human knee. The trajectories were calculated with a method based on nonlinear parameter optimization (Buschmann et al., 2005).

The biped robot *BIP 2000* (Espiau and Sardain, 2000) employs linear actuators in the knees, however, the kinematics are different from the proposed mechanism: A satellite roller screw is fixed to the shank, and connected to the knee with a steering rod. An additional linear bearing is required to keep the satellite roller screw free from radial loads.

7-DoF legs with toe joints Nearly all humanoid robots including *JOHNNIE* are designed with 6-DoF legs—3 DoF in the hip, one in the knee and two in the ankle. Each foot consists of one rigid body, therefore heel lift-off during terminal stance phase can hardly be realized. Even small disturbances lead to instabilities due to the line contact of the foot's leading edge with the floor. In human walking heel lift-off of the stance leg occurs during terminal swing, i. e. shortly before the swing leg has floor contact (Perry, 1992). For biped robots with one-piece foot segments forward roll across the forefoot constitutes an underactuated, marginally stable state and is therefore not performed during normal walking. Especially for larger step lengths, this leads to an extended knee configuration at initial contact of the swing leg, resulting in large joint accelerations.

Therefore an additional link between forefoot and heel equivalent to the human toes is proposed. Heel lift-off in the stance leg allows the swing leg to be in a more extended configuration. Area contact of the toe segment stabilizes the robot and facilitates forward roll across the forefoot which is expected to reduce the joint loads in hip and knee compared to a 6-DoF leg configuration. To our knowledge the only humanoids with actively driven toe joints are *H6* and *H7* (Nishiwaki et al. 2002a), and there are only few robots with passive toe joints.

DESIGN OF ROBOT HARDWARE

Dimensioning of the robot hardware is an iterative process of mechanical design and extensive multibody simulations (Pfeiffer, 2004). Kinematics, geometrical data and gear transmission ratios, together with body masses and inertia obtained from the 3D-CAD model of the robot serve as input parameters for the dynamic simulation of the system (cf. "DYNAMIC SIMULATION"). The most important parameters obtained from the simulation are the joint torques and angular velocities used for motor and gear selection, and the constraint forces acting on the robot's links to be used for Finite Element simulations.

Selection of the actuators is a demanding task because they must be able to move at high velocity while good dynamic performance is required to accelerate the links. On the other hand, for minimal weight of the robot it is essential not to oversize the drives while at the same time appropriate power reserves should be kept. Three major demands on the actuators are (1) high dynamic response, (2) high output axis speed and (3) high output axis torque over a large speed range.

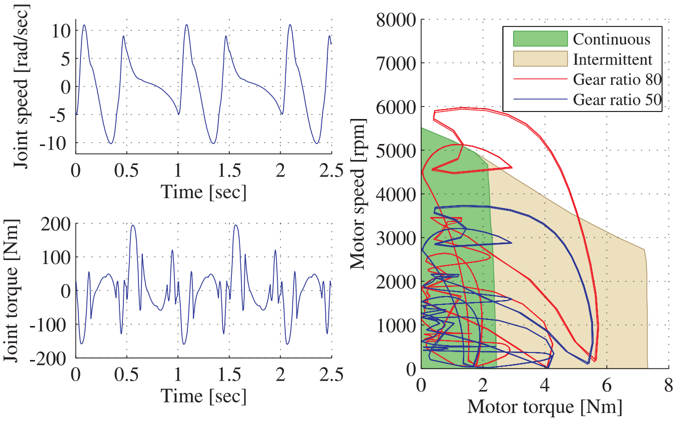

Figure 5 – Torque and speed requirements of the hip joint pitch axis and torque speed diagram of the motor

Figure 5 exemplifies motor and gear selection for the hip joint pitch axis of *LOLA* on the basis of a stable gait pattern at a walking speed of 5 km/h (Buschmann et al., 2005). From the right hand plot it can be seen that the torque demands for gear ratios of $N = 80$ and $N = 50$ are similar. However, the higher motor speed at $N = 80$ means that the motor torque is mainly spent on accelerating the motor shaft. For $N = 50$ a motor with less power (and weight) can be chosen, which is shown by the shaded areas representing the motor characteristic for continuous and intermittent operation. Thus, drive efficiency, denoted by the ratio of load moment and motor shaft acceleration torque, can be increased because the torque and speed bandwidths of the employed motors permit smaller gear ratios.

MODULAR JOINT CONCEPT FOR *LOLA*

Obviously, a modular structure of the whole robot would be desirable from the manufacturing and maintenance point of view. However, a fully modular structure would lead to higher weight and suboptimal mass distribution. The detailed

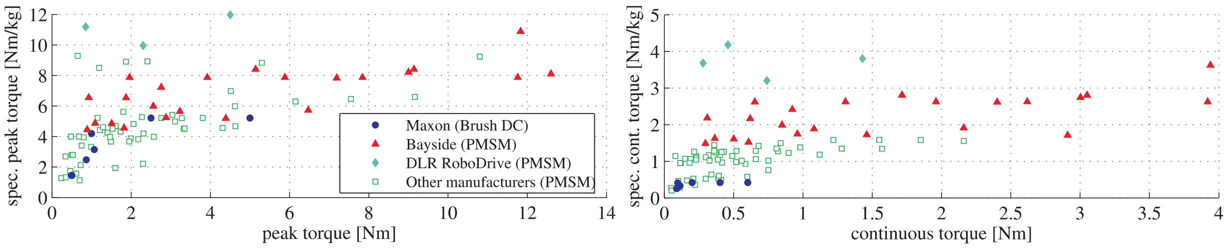

Figure 6 – Comparing the power density of commercially available DC motors and PMSM

analysis in Gienger, 2005, reveals that structural components contribute 43 % to *JOHNNIE*'s weight. With approximately 31 % the drive chains make the second largest part—22.7 % account for the motors and another 7.9 % for the gears, making the development of compact and lightweight joint units a crucial factor.

The main structure of the robot is non-modular with joints that are built on the unit construction principle. They have identical structure with the sizes of gear and motor adapted to the requirements of each link. Many parts are standardized for all drives, but some housings are specialized to minimize weight and to achieve an optimal load spread and distribution. This turned out to be the most reasonable way to design the robot at minimal weight while taking into account ease of manufacturing. There are only 7 different drives for the 22 actuated DoF of *LOLA*.

To realize such highly integrated joint units with maximum power density it is necessary to use the latest technologies in the field of electrical drives, gears and sensors. Currently, the predominant actuation principle for humanoid robots is a combination of Harmonic Drive gears and DC brush motors, mostly coupled with timing belts (Nishiwaki et al., 2002b, Kaneko et al., 2004, Ogura et al., 2004, Kim et al., 2005). For *ASIMO* (Honda, 2005) and *ETL-HUMANOID* (Nagakubo et al., 2001) both DC brush motors and DC brushless motors drive the joints through Harmonic Drive gears. *JOHNNIE* is actuated by DC brush motors and Harmonic Drive gears, except for the ankle joints that are driven by parallel mechanisms with ballscrews (Gienger, 2001). The robot *BIP 2000* (Espiau and Sardain, 2000) is equipped with brushless motors and Harmonic Drive gears or satellite roller screws.

For *LOLA* we use high performance brushless motors from Parker Bayside because of their superior torque and speed capabilities. Linear drives based on ballscrews are used in knee and ankle joints, all other joints employ Harmonic Drive gears as speed reducers. Each drive unit contains an incremental rotary encoder, an absolute angular encoder as link position sensor and a light barrier as limit switch. The fusion of motor, gear and sensors into a highly integrated, mechatronic joint module has several advantages for the whole system:

- High velocity range at good dynamic performance,
- high power density, i.e. high efficiency,
- comparatively small volume of the whole drive unit,
- reliability due to brushless design of the motors and the capability of self-monitoring and diagnosis.

The main reasons for us to choose permanent magnet synchronous motors (PMSM) over DC brush motors for *LOLA* are robustness, a significantly higher power density, and higher torque and speed bandwidths. Figure 6 compares the performance data of commercially available DC brush motors and PMSM. Obviously, PMSM are superior to DC brush motors in both specific peak and continuous torque. However, control algorithms and power electronics are more complex because of electronic commutation and three-phase design. PMSM permit larger stall torques for longer intervals than DC motors where mechanical commutation severely limits stall torque. This is especially important for slow motions or when the robot is standing, i. e. when the motors are in reversing operation around zero speed or joint positions are held for a certain time. A special type of PMSM are *frameless motors* which consist of a stator lamination stack with three-phase winding plus a rotor with permanent magnets bonded onto a ferrous tube. Motor shaft and bearing have to be custom-made which facilitates a space-saving integration directly into the joint. There is no need for couplings or timing belts, making the whole drive chain free from backlash and slip and, ultimately, increases stiffness and system bandwidth. For optimal heat transfer the joint housing has cooling fins and the stator is bonded into the housing with a thermally conductive adhesive. Additional forced ventilation is employed in the highly loaded knee and hip joints. The joint design is given in greater detail in Lohmeier et al., 2006.

DYNAMIC SIMULATION

Design and sizing of the robot's mechanical and electronic components must be based on comprehensive simulation data. Similarly, development of the control and trajectory generation system and dynamics analysis require a simulation model capable of accurately predicting all physical phenomena of interest. To this end we implemented a modular simulation system that can be used to simulate various robot configurations during development. Figure 7 shows the logical

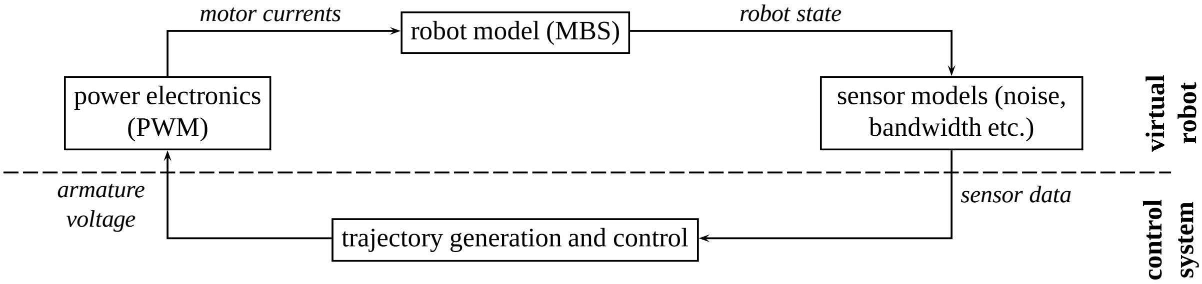

Figure 7 – Schematic representation of the simulation system.

structure of the simulation system. The modules shown in the top half of the diagram simulate the sensors, actuators, power electronics and dynamics, i.e. the robot hardware. The module "trajectory generation and control" implements the entire robot control. The simulation system and the real robot provide source-level compatible interfaces for sensor data acquisition and control commands. Thus the simulation environment allows to safely test unmodified controller code in a virtual environment prior to conducting experiments.

LOLA's and *JOHNNIE*'s links are made of aluminum and designed for high stiffness. Therefore, the robot is modeled as a rigid multibody system (MBS). The equations of motion (EOM) are calculated in minimal coordinates using the NEWTON-EULER formalism and written in the following form:

$$\mathbf{M}\ddot{\mathbf{q}} + \mathbf{h}(\mathbf{q}, \dot{\mathbf{q}}) = \mathbf{Q}_{\text{mot}} + \mathbf{Q}_{\text{gear}} + \mathbf{Q}_{\text{cont}} \tag{1}$$

$$\mathbf{L}\dot{\mathbf{I}} = -\mathbf{R}\mathbf{I} - \mathbf{k_M}\dot{\varphi} + \mathbf{U} \tag{2}$$

where $\mathbf{q}$ are the generalized coordinates, $\mathbf{M}$ the mass matrix and $\mathbf{h}$ the vector of Coriolis forces, centrifugal forces etc. Therefore, the left hand side of (1) takes into account all effects due to rigid body mechanics, including nonlinear ballscrew drive mechanisms etc., while the remaining generalized forces are given on the right hand side. $\mathbf{Q}_{\text{mot}}$ are the forces due to motor torques, $\mathbf{Q}_{\text{gear}}$ generalized gear friction forces and $\mathbf{Q}_{\text{kont}}$ forces due to foot-ground contact. Equation (2) describes the electrical dynamics of the robot's motors. In case of PMSM motors, the equations hold for the coordinate system fixed to the motor shaft. $\mathbf{L}$ denotes the inductance, $\mathbf{R}$ the armature resistance, $\mathbf{k_M}$ the torque constant, $\mathbf{I}$ the motor currents and $\mathbf{U}$ the applied voltage. The modeling procedure is explained in more detail in Buschmann, 2006.

Experimental Verification

In order to verify modeling assumptions, we performed walking experiments with *JOHNNIE* and implemented a simulation model using the software framework described above. Figure 8 shows the normal reaction force acting on one foot measured during the experiment and the corresponding results from a detailed and a simplified simulation model. The detailed simulation includes nonlinear friction models for the Harmonic Drive gears and ballscrews, effects due to the nonlinear ballscrew drive mechanisms and the motor's electrical dynamics. Using this model, all relevant effects can be predicted with sufficient accuracy. In order to reduce simulation times, a simplified model with shorter integration times was implemented. The simplified model does not include such effects as drive friction, but still predicts global system dynamics quite accurately as shown in Fig. 8. More detail on the two simulation models is given in Buschmann, 2006.

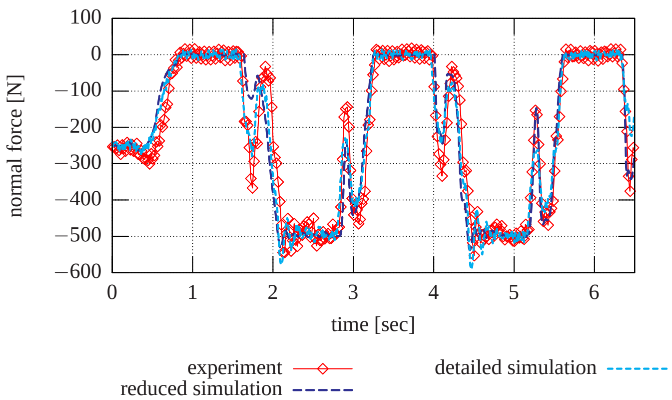

Figure 8 – Normal force acting on *JOHNNIE*'s right foot during an experiment and simulation results.

MODULAR COMPUTER SYSTEM

With 22 actuators and several sensors not mentioned above (e. g. force/torque sensors, attitude sensor) *LOLA* is a rather complex system. A decentral electronics architecture would complement the modular joint concept and would be preferable in order to decrease complexity, to simplify first-time operation and to make the system expandable for additional degrees of freedom or sensors. Unfortunately, a fully decentral controller architectures is not suitable for humanoid robots due to the highly coupled dynamics. However, it is possible and reasonable to shift low-level control of joint positions and velocities to local controllers. The field-orientated control algorithms for brushless motors are computationally more expensive than controllers for DC motors. In our robot *LOLA* the central system controller is unloaded from these standard tasks, and motor control is executed in parallel on the embedded controllers.

The proposed modular electronics system makes custom hardware necessary for the embedded controllers because of the combination of interfaces, comprising communication bus, absolute angular encoder and other sensors. However, off-the-shelf components will be used for the central system controller. An industrial PC board supplemented by an interface board for the communication bus turns out to be the most efficient solution, as it provides enough computational power and can be upgraded easily.

For a decentral architecture, bus systems for both power and communication replace the complex, bulky cabling of a central system where cables contribute 4.7 % to the total weight (Gienger, 2005). The major requirements on the communication bus employed between central system controller and local controllers include

- Real-time capability and a high level of determinism,
- guaranteed bandwidth with minimal protocol overhead.

Compared to an IEEE 1394-based solution, different implementations of real-time Ethernet and CAN, a SERCOS-III-based system turned out to be the best solution. SERCOS-III is a digital communication interface based on Ethernet physics for communication of standardized closed-loop data in real-time. It provides an accurately timed, high speed serial interface (max. 100 MBaud) and is about to be adopted as an international standard (IEC/PAS 62410, 2005). The SERCOS-III protocol defines both cyclic communication within deterministic time slices for real-time communications and a non-cyclic channel for non-real-time data transfers such as status and diagnostic messages. The non-cyclic channel also facilitates parametrization of the drives, switching between different operating modes and gain scheduling.

CONCLUSION AND OUTLOOK

Despite recent advances walking machines are still slow compared to biological systems and have limited autonomy. The intention of the research presented is to diminish this gap. In comparison to *JOHNNIE*, the new robot *LOLA* features a modular, multisensory joint design with brushless motors. The electronics architecture is designed as an “intelligent sensor-actuator network with a central controller”. The new decentral components increase the system’s performance from a technological point of view. Additional DoFs are introduced to allow for more flexible and natural motions. The trajectory generation and control system is currently being developed, aiming for faster, more flexible and more robust walking patterns. The control system features a gait pattern adaptation scheme inspired by that observed in human walking. Nevertheless, we are just at the beginning of taking advantage of biological findings and transferring some of the observed principles to technological systems. This transfer promises significant advantages for the sciences involved. At the same time it poses a great challenge and requires further interdisciplinary research by scientists from biology, medicine and engineering.

ACKNOWLEDGMENTS

This work is supported by the “Deutsche Forschungsgemeinschaft” (Project UL 105/28).

REFERENCES

Buschmann, T., Lohmeier, S., Ulbrich, H. and Pfeiffer, F., “Optimization based gait pattern generation for a biped robot,” in *Proc. Int. Conf. Humanoid Rob. (Humanoids)*, Tsukuba, Japan, 2005.

Buschmann, T., Lohmeier, S., Ulbrich, H. and Pfeiffer, F., “Modeling and simulation of a biped robot,” in *Proc. IEEE Int. Conf. Rob. Aut. (ICRA)*, Orlando, USA, 2006.

Espiau, B. and Sardain, P., “The anthropomorphic biped robot BIP 2000,” in *Proc. IEEE Int. Conf. Rob. Aut. (ICRA)*, San Francisco, USA, 2000, pp. 3997–4002.

Gienger, M., “Entwurf und Realisierung einer zweibeinigen Laufmaschine”, ser. Fortschrittberichte VDI, Reihe 1. Düsseldorf: VDI-Verlag, 2005, no. Nr. 378.

Gienger, M., Löffler, K. and Pfeiffer, F., “Towards the design of a biped jogging robot,” in *Proc. IEEE Int. Conf. Rob. Aut. (ICRA)*, Seoul, Korea, 2001, pp. 4140–4145.

Hirai. K, Hirose. M, and Takenaka. T, "The development of Honda humanoid robot," in *Proc. IEEE Int. Conf. Rob. Aut. (ICRA)*, Leuven, Belgium, 1998, pp. 1321–1326.

Hirzinger. G, Sporer. N, Albu-Schäffer, A., Hähnle, M., Krenn. R, Pascucci. A, and Schedl. M, "DLR's torque-controlled light weight robot III – are we reaching the technological limits now?" in *Proc. IEEE Int. Conf. Rob. Aut. (ICRA)*, vol. 2, Washington, DC USA, 2002, pp. 1710–1716.

Honda Motor Co., Ltd., (2005, Dec), "New ASIMO - running at 6km/h." [Online]. Available: `http://world.honda.com/HDTV/ASIMO/New-ASIMO-run-6kmh/`

Ishida. T, Kuroki. Y, and Yamaguchi. J, "Mechanical system of a small biped entertainment robot," in *Proc. IEEE/RSJ Int. Conf. Rob. Sys. (IROS)*, 2003, pp. 1129–1134.

Kajita. S, Nagasaki. T, Kaneko. K, K. Yokoi, and K. Tanie, "A hop towards running humanoid biped," in *Proc. IEEE Int. Conf. Rob. Aut. (ICRA)*, 2004, pp. 629–635.

Kaneko. K, Kanehiro. F, Kajita. S, Hirukawa. H, Kawasaki. T, Hirata. M, Akachi. K, and Isozumi. T, "Humanoid robot HRP-2," in *Proc. IEEE Int. Conf. Rob. Aut. (ICRA)*, New Orleans, USA, 2004, pp. 1083–1090.

Kim, J.-Y., Park, I.-W., Lee. J, Kim, M.-S., Cho, B.-K. and Oh,J.-H., "System design and dynamic walking of humanoid robot KHR-2," in *Proc. IEEE Int. Conf. Rob. Aut. (ICRA)*, 2005, pp. 1443–1448.

Lohmeier. S, Buschmann. T, Ulbrich. H, and Pfeiffer. F, "Modular joint design for a performance enhanced humanoid robot," in *Proc. IEEE Int. Conf. Rob. Aut. (ICRA)*, Orlando, USA, 2006.

Nagakubo. A, Kuniyoshi. Y, and Cheng. G, "ETL-humanoid–a high-performance full body humanoid system for versatile actions," in *Proc. IEEE/RSJ Int. Conf. Rob. Sys. (IROS)*, 2001, pp. 1087–1092.

Nishiwaki, K., Kagami, S., Kuniyoshi, Y., Inaba, M. and Inoue, H., "Toe joints that enhance bipedal and fullbody motion of humanoid robots," in *Proc. IEEE Int. Conf. Rob. Aut. (ICRA)*, Washington, USA, 2002, pp. 3105–3110.

Nishiwaki. K, Kagami. S, Kuffner. J, Inaba. M, and Inoue. H, "Humanoid "JSK-H7": Research platform for autonomous behavior and whole body motion," in *Proc. Int. Workshop Humanoid and human friendly Robotics (IARP)*, Tsukuba, Japan, 2002, pp. 2–9.

Ogura, Y., Aikawa, H., Lim, H.-O. and Takanishi, A, "Development of a human-like walking robot having two 7-DOF legs and a 2-DOF waist," in *Proc. IEEE Int. Conf. Rob. Aut. (ICRA)*, 2004, pp. 134–139.

Perry,J.,"Gait Analysis – Normal and Pathological Function", 1992.

Pfeiffer. F, "Technical aspects of walking," in "Walking: Biological and Technical Aspects (CISM Courses and Lectures)", ser. CISM Courses and Lectures, Pfeiffer. F and Zielinska. T, Berlin, Heidelberg, New York: Springer, 2004, vol. 467, pp. 119–153.

Pfeiffer. F, Löffler, K., Gienger. M, and H. Sensor, "Ulbrich and control aspects of biped robot "Johnnie"," *International Journal of Humanoid Robotics (IJHR)*, vol. 1, no. 3, pp. 481–496, 2004.

IEC/PAS 62410, "Real-time Ethernet SERCOS III", Sep. 2005.

RESPONSIBILITY NOTICE

The author(s) is (are) the only responsible for the printed material included in this paper.